

Giant quadrupole resonance in Ni isotopes

D. H. Youngblood and Y.-W. Lui

Texas A&M University, College Station, Texas 77843

U. Garg

University of Notre Dame, South Bend, Indiana 46556

R. J. Peterson

University of Colorado, Boulder, Colorado 80309

(Received 14 October 1991)

Inelastic scattering of 129 MeV alpha particles has been used to excite the giant quadrupole resonance in $^{58,60,62,64}\text{Ni}$. The resonance was found to exhaust $58\pm 12\%$, $76\pm 14\%$, $78\pm 14\%$, and $90\pm 16\%$ of the $E2$ energy-weighted sum rule, respectively, for $^{58,60,62,64}\text{Ni}$.

PACS number(s): 25.55.Ci, 24.30.Cz, 27.50.+e

INTRODUCTION

The energy, width, and transition strength of the giant quadrupole resonance (GQR) in ^{58}Ni have been determined in a number of studies [1–9] by different groups with a variety of projectiles. However, information on the GQR in the other Ni isotopes is limited. Oakley *et al.* [10] studied $^{58,60,62,64}\text{Ni}$ with pions but reported large uncertainties for both excitation energy and width for the GQR and isoscalar transition strength exceeding the sum rule in $^{62,64}\text{Ni}$ using a collective model. Gulkarov [2] Youngblood *et al.* [3], and Buenerd *et al.* [4] have studied the GQR in ^{60}Ni , but Gulkarov, using electron scattering, obtains an excitation energy more than 3 MeV below the other reports. Knopfle *et al.* [11] discuss decay of the GQR in ^{62}Ni but do not report the excitation energy, width, or strength. Garg *et al.* [8] and Gulkarov [2] report parameters for ^{64}Ni , but the excitation energies differ by more than 2 MeV. Neither reported the strength of the resonance.

Therefore, we have explored the giant resonance regions of the Ni isotopes 58, 60, 62, and 64 with inelastic scattering of 129 MeV alpha particles over the angle range 4° – 17° to establish the parameters of the GQR in the three heavier nuclei. ^{58}Ni was measured in the same experimental run in order to provide a systematic measurement over the isotopic series to reduce errors due to calibrations, differing beam energies, etc. This work also permits a comparison of the isoscalar transition strengths to those obtained from the pion work [10].

EXPERIMENTAL PROCEDURE

Inelastically scattered spectra were measured for 129 MeV alpha particles obtained from the Texas A&M University variable energy cyclotron. The experimental setup and beam preparation methods were similar to those described in detail in Ref. [12] and are only summarized below. Considerable care was taken to minimize spurious contributions from the beam as well as slit scattering.

Runs with blank target frames were taken to ascertain that contributions from such processes were negligible in regions of interest. Target thicknesses and the angles at which data were taken are shown in Table I. All targets were foils enriched to $>98\%$ in the isotope of interest. Their thicknesses were measured with an Am alpha source using the energy-loss method. The inelastically scattered alpha particles were detected in the focal plane of the Enge split-pole spectrograph with a 40 cm long resistive wire proportional counter backed by an NE102 plastic scintillator. The solid angle defining slits were set at $\pm 0.3^\circ$ horizontally and $\pm 0.9^\circ$ vertically. Details of the electronic setup, the data acquisition system, and techniques for estimating the continuum under the peaks are discussed in Ref. [12]. Energy calibrations were obtained from inelastic scattering from a 1 mg/cm² carbon foil over the angle range 4° – 17° .

The distorted-wave Born approximation (DWBA) calculations used a collective derivative transition potential and are discussed in detail in Refs. [6,12]. Optical parameters determined from $^{58}\text{Ni} + \alpha$ elastic scattering [3] at 96 MeV were used for all DWBA calculations. Calculations were averaged over the finite angle opening of the detector. A least-squares peak fitting program using linearization techniques to fit multiple peaks in multiple spectra simultaneously was used to fit the data in the giant resonance region. This program runs on 80386-80486 class computers using Microsoft Fortran and a Grafmatic graphics package from Microcompatibles, Inc. The pro-

TABLE I. Experimental parameters for Ni runs.

Isotope	Target thickness (mg/cm ²)	Angles taken laboratory (deg)
58	4.18	3.77,6.77,12.77,16.77
60	0.99	3.77,5.77,7.52,12.77,16.77
62	1.85	3.77,5.77,7.52,12.77,16.77
64	1.64	3.77,4.77,5.77,6.77,7.52,12.77,16.77

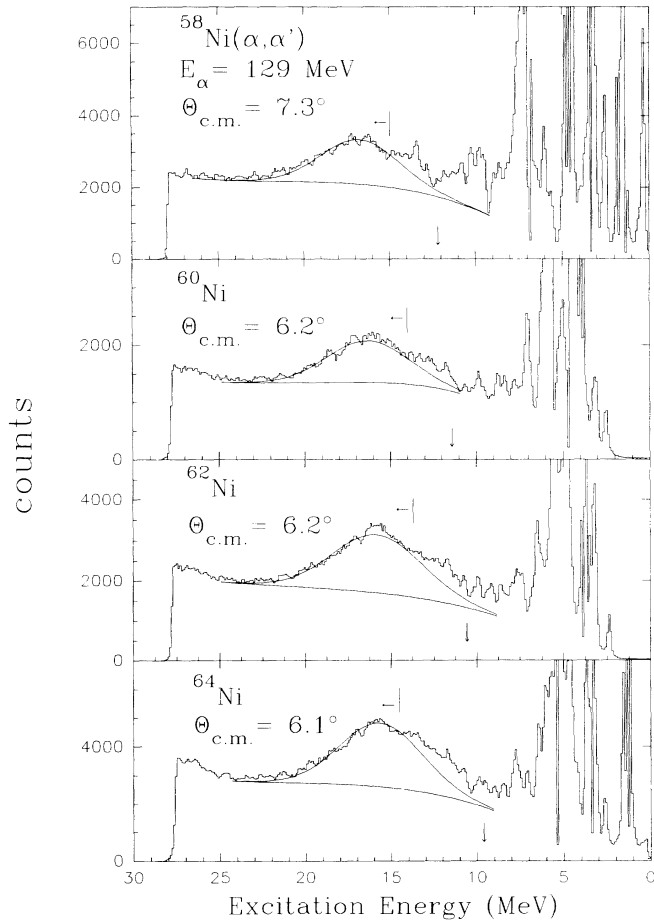


FIG. 1. Sample spectra for 129 MeV inelastic alpha scattering from each isotope showing the estimated continuum and a Gaussian representing the GQR. The neutron binding energy is indicated by the vertical arrow in each spectrum. The lower E_x limit used for the fits to the GQR is indicated by the vertical line and left arrow at $E_x \approx 14$ MeV for each spectrum.

gram has been modified from an earlier version [12] for better convergence, convenient interactive input, and output compatibility with standard personal computer spreadsheets for manipulation, evaluation, and display of results.

EXPERIMENTAL RESULTS

Sample spectra obtained for each of the nuclei are shown in Fig. 1. Also illustrated is the estimated continuum under the giant resonance peak. As can be seen, the

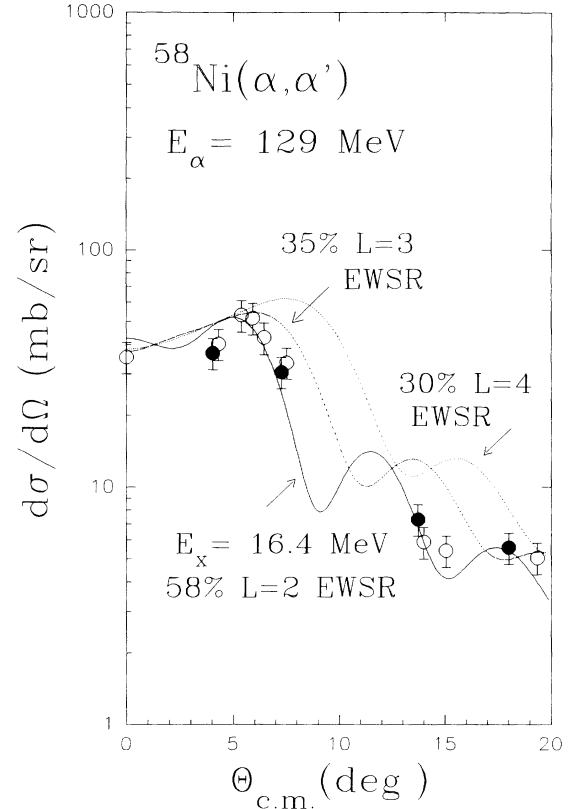


FIG. 2. The angular distribution obtained for the GQR peak in ^{58}Ni is shown by the solid circles. The estimated uncertainties are approximately the size of the points. Data points previously reported [9] are shown by the open circles. DWBA calculations for $L=2, 3$, and 4 normalized as indicated are shown by the solid, dashed, and dot-dashed lines, respectively.

GQR in the Ni isotopes has fine structure on the low excitation energy side, and two sets of fits were carried out. One set fit the entire peak including fine structure for each isotope using several narrow peaks in addition to the broad giant resonance (e.g., three narrow and one broad in ^{58}Ni), while in the second set the fit region was chosen to begin at an excitation energy above the fine structure. The parameters obtained for the GQR with each technique were very similar, and the fits to the peaks in the lower region were not definitive.

For ^{58}Ni and ^{60}Ni , the widths and positions obtained for the GQR at each of the angles were very similar, and quite good fits were obtained by requiring the same energy and width in each spectrum. For ^{62}Ni and ^{64}Ni , however, the peak position and width were clearly different at

TABLE II. GQR parameters. Errors in energy and width do not include systematic errors.

Isotope	E_x (MeV)	Γ (MeV)	$(\beta R)^2$	$E2$ EWSR (%)	C_0
58	16.49 ± 0.10	5.37 ± 0.25	0.53	58 ± 12	0.80 ± 0.04
60	16.31 ± 0.13	5.89 ± 0.25	0.68	76 ± 14	0.84 ± 0.04
62	15.81 ± 0.40	6.38 ± 0.80	0.69	78 ± 14	0.82 ± 0.12
64	15.60 ± 0.30	5.63 ± 0.40	0.78	90 ± 16	1.05 ± 0.10

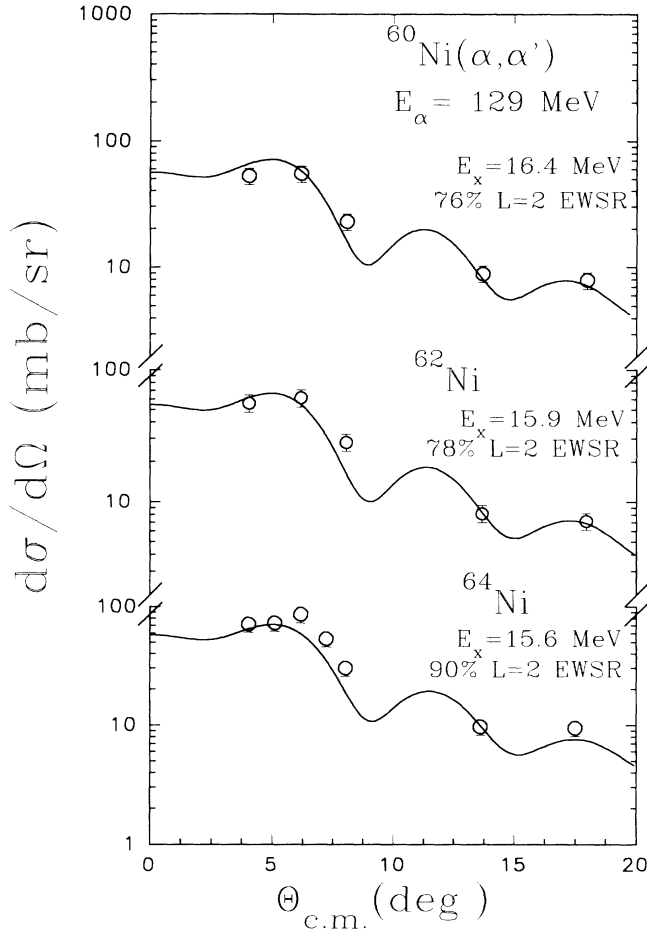


FIG. 3. Angular distributions obtained for the GQR peak for $^{60,62,64}\text{Ni}$. The estimated uncertainties are approximately the size of the points. DWBA calculations normalized according to the βR shown in Table II are shown by the lines.

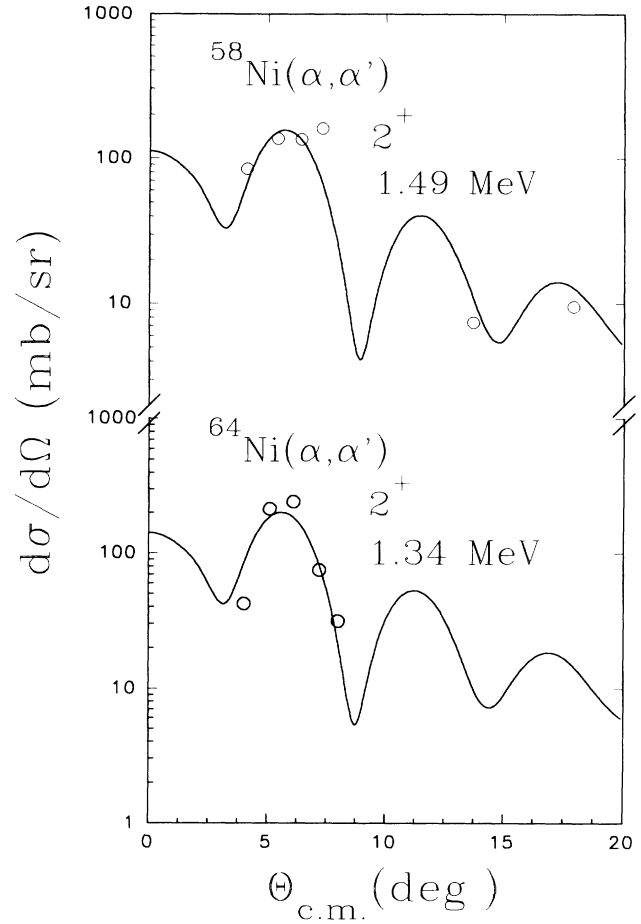


FIG. 4. Angular distributions obtained for low-lying 2^+ states in $^{58,64}\text{Ni}$. The solid lines represent DWBA calculations for $l=2$ transfer normalized according to the βR shown in Table IV.

TABLE III. Comparison with other work. Errors for this work include systematic errors.

Isotope	E_x (MeV)	Γ (MeV)	$E2$ EWSR (%)	Reference
58	16.5 ± 0.3	5.4 ± 0.3	58 ± 12	This work
	16.1 ± 0.2	4.7 ± 0.2	52 ± 10	[9]
	16.4 ± 0.2	4.3 ± 0.2	38 ± 8	[7]
	16.9 ± 0.2	4.9 ± 0.2	55 ± 15	[3]
	15.7 ± 0.2	4.2 ± 0.2		[8]
	13.7 ± 0.3	4.7 ± 0.3		[2]
	16.4 ± 1	6.8 ± 1	126 ± 22	[10]
60	16.4 ± 0.2	5.9 ± 0.3	76 ± 14	This work
	16.6 ± 0.3	5.0 ± 0.4	63 ± 15	[3]
	15.9 ± 0.3	5.0 ± 0.4	53	[4]
	13.0 ± 0.3	4.1 ± 0.3		[2]
	16.4 ± 1	6.8 ± 1	112 ± 23	[10]
62	15.9 ± 0.4	6.4 ± 0.8	78 ± 14	This work
	16.4 ± 1	6.8 ± 1	221 ± 31	[10]
64	15.6 ± 0.3	5.6 ± 0.4	90 ± 16	This work
	15.4 ± 0.2	4.2 ± 0.2		[8]
	13.2 ± 0.3	4.8 ± 0.3		[2]
	16.4 ± 1	6.8 ± 1	170 ± 23	[10]

TABLE IV. Low-lying states.

Isotope	E_x (MeV)	This work		Other work
		βR	J^π	βR
58	1.49	0.86	2^+	0.94, ^a 0.87, ^b 1.02 ^c
	4.48	0.68	3^-	0.73 ^c
60	4.01	0.73	3^-	0.81 ^c
62	3.78	0.75	3^-	0.75 ^d
64	1.34	0.96	2^+	0.90 ^d
	3.53	0.78	3^-	0.79 ^d

^aReference [3].^bReference [14].^cReference [16].^dAverage values from Ref. [15].

some angles, as if additional components with different L 's were present. The discrete peaks observed in $^{62,64}\text{Ni}$ (up to about $E_x = 9$ MeV) are in agreement in position for all the spectra, suggesting that the apparent position variations in the giant resonance peak are not instrumental. Consequently, for $^{62,64}\text{Ni}$, each spectrum was fit separately and the widths and positions averaged. The energies and widths obtained from the fits to the region above the fine structure are given in Table II. The errors quoted for $^{58,60}\text{Ni}$ are those uncertainties in the fitting process (diagonal element of error matrix), whereas those for $^{62,64}\text{Ni}$ are the standard deviations calculated from the values obtained for each spectrum separately. Systematic errors are not included in Table II. A Gaussian peak calculated from the parameters in Table II for one spectrum for each nucleus is shown in Fig. 1.

The angular distribution obtained for ^{58}Ni along with the $L=2, 3$, and 4 calculations are shown in Fig. 2. Angular distributions obtained for the other nuclei are shown in Fig. 3 along with $L=2$ DWBA calculations. The $L=2$ calculations fit the data well for all nuclei, suggesting that most of the strength is quadrupole. The drop in the cross section for each of the nuclei at 8° is consistent only with the $L=2$ calculation. While a monopole resonance would also exhibit this drop in cross section at 8° , over the angle range covered in this work, a monopole resonance of the strength observed [7,9] in ^{58}Ni would contribute less than 5% of the cross section in the region fitted. Also shown for ^{58}Ni are the cross sections for the GQR measured in an earlier experiment [9], where the monopole resonance at 17.0 MeV was subtracted. These are in excellent agreement with the present data.

DISCUSSION

Table III contains a comparison of the results of this work with other results for the Ni isotopes. For ^{58}Ni , only the more recent results are shown except in those cases where other Ni isotopes were also reported. It is immediately apparent that the excitation energies reported by Gulkarov for $^{58,60,64}\text{Ni}$ are lower than the other results by 2 MeV or more. Otherwise the results are in reasonable agreement, with excitation energies and widths being generally within one standard deviation of

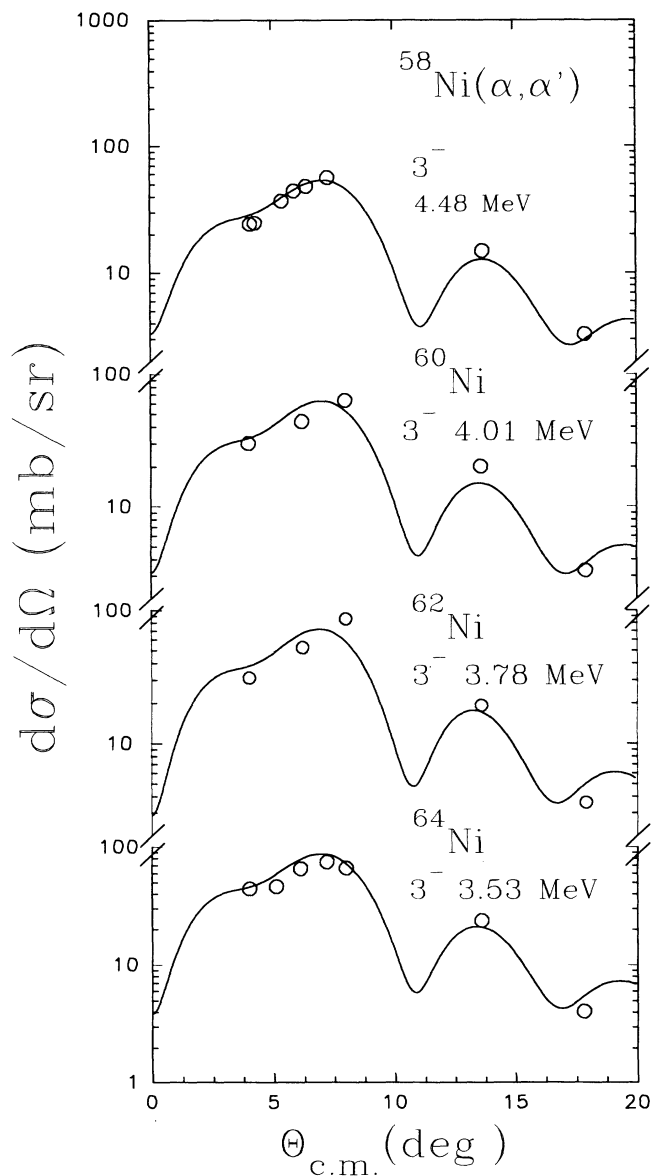


FIG. 5. Angular distributions obtained for low-lying 3^- states in each isotope. The solid lines represent DWBA calculations for $l=3$ transfer normalized according to the βR shown in Table IV.

the average, particularly for ^{58}Ni where numerous measurements exist. For ^{60}Ni , this work is in reasonable agreement both with early 96 MeV alpha work [3] and with ^3He scattering [4]. For ^{64}Ni , the excitation energy obtained in this work is in agreement with that from ^{14}N scattering [8], but the width obtained here is considerably greater. The strengths obtained from the isoscalar analysis of the pion work [10] are systematically much larger than other values.

Loveman and Peterson [13] noted that the width and centroid of the giant quadrupole resonance vary in a simple way with the neutron binding energy:

$$E_x - S_n = C_0 \Gamma,$$

where S_n is the neutron separation energy and C_0 is an empirical constant. The values of C_0 obtained from our data are shown in Table II. For $^{62,64}\text{Ni}$ the values are consistent with 1.0; however, for $^{58,60}\text{Ni}$ they are somewhat lower. The difference in C_0 values for ^{58}Ni and ^{64}Ni is much less than found in the ^{14}N scattering [8].

In ^{58}Ni and ^{64}Ni the first excited state and a strong collective 3^- state around $E_x = 4$ MeV were analyzed also. For ^{60}Ni and ^{62}Ni , the first excited state was at least partially blocked from the detector by a plate which prevented elastic scattering from entering the detector, and only the strong 3^- state could be extracted. The overall energy resolution was approximately 120 keV, so the 3^- state was not completely separated from nearby states. The angular distributions obtained for these states are shown with DWBA calculations superimposed in Figs. 4 and 5. The excitation energies and βR values extracted are shown in Table IV. The strengths and energies obtained are generally in good agreement with other results.

ACKNOWLEDGMENTS

This work was supported in part by the Robert A. Welch Foundation and by the U.S. Department of Energy under Grant No. DE-FG05-86ER40256.

-
- [1] M. Buenerd, J. Phys. C **4**, 115 (1984).
 - [2] I. S. Gulkarov, Yad. Fiz. **20**, 17 (1974) [Sov. J. Nucl. Phys. **20**, 9 (1975)].
 - [3] D. H. Youngblood, J. M. Moss, C. M. Rozsa, J. D. Bronson, A. D. Bacher, and D. R. Brown, Phys. Rev. C **13**, 994 (1976).
 - [4] M. Buenerd, C. Bonhomme, D. Lebrun, P. Martin, J. Chauvin, G. Duhamel, G. Perrin, and P. de Saintignon, Phys. Lett. **84B**, 305 (1979).
 - [5] F. E. Bertrand, G. R. Satchler, D. J. Horen, and A. van der Woude, Phys. Lett. **80B**, 198 (1979); F. E. Bertrand, G. R. Satchler, D. J. Horen, J. R. Wu, A. D. Bacher, G. T. Emery, W. P. Jones, D. W. Miller, and A. van der Woude, Phys. Rev. C **22**, 1832 (1980).
 - [6] D. H. Youngblood, P. Bogucki, J. D. Bronson, U. Garg, Y.-W. Lui, and C. M. Rozsa, Phys. Rev. C **23**, 1997 (1981); U. Garg, P. Bogucki, J. D. Bronson, Y.-W. Lui, C. M. Rozsa, and D. H. Youngblood, *ibid.* **25**, 3204 (1982).
 - [7] G. Duhamel, M. Buenerd, P. de Saintignon, J. Chauvin, D. Lebrun, Ph. Martin, and G. Perrin, Phys. Rev. C **38**, 2509 (1988).
 - [8] U. Garg, K. B. Beard, D. Ye, A. Galonsky, T. Murakami, J. S. Winfield, Y.-W. Lui, and D. H. Youngblood, Phys. Rev. C **41**, 1845 (1990).
 - [9] D. H. Youngblood and Y.-W. Lui, Phys. Rev. C **44**, 1878 (1991).
 - [10] D. S. Oakley, M. R. Braunstein, J. J. Kraushaar, R. A. Loveman, R. J. Peterson, D. J. Rilett, and R. L. Boudrie, Phys. Rev. C **40**, 859 (1989).
 - [11] K. T. Knöpfle, H. Riedesel, K. Schindler, G. J. Wagner, C. Mayer-Böricke, W. Oelert, M. Rogge, and P. Turek, J. Phys. G **7**, L99 (1981).
 - [12] C. M. Rozsa, D. H. Youngblood, J. D. Bronson, Y.-W. Lui, and U. Garg, Phys. Rev. C **21**, 1252 (1980).
 - [13] R. A. Loveman and R. J. Peterson, Z. Phys. A **328**, 281 (1987).
 - [14] M. Buenerd, K. Bouhelel, Ph. Martin, J. Chauvin, D. Lebrun, G. Perrin, P. de Saintignon, and G. Duhamel, Phys. Rev. C **38**, 2514 (1988).
 - [15] R. L. Auble, Nucl. Data Sheets **28**, 103 (1979); M. L. Halbert, *ibid.* **26**, 5 (1979); **28**, 179 (1979).
 - [16] O. N. Jarvis, B. G. Harvey, D. L. Hendrie, and Jeanette Mahoney, Nucl. Phys. A **102**, 625 (1967).